Supporting Information

Magnetic delivery and ultrasound-responsive release of chelating microcapsules for selective removal of urolithiasis

Byung Kwon Kaang[a], Sunjae Lee[a], JunJie Piao[b], Hyuk Jin Cho[b*], and Dong-Pyo Kim[a*]

Experimental section

Materials

Sodium hexametaphosphate (HMP, 96 %, crystalline), ethylenediaminetetraacetic acid (EDTA, 99.4-100.6%, powder), sodium citrate ($HOC(COONa)(CH_2COONa)_2 \cdot 2H_2O$), dichloromethane (DCM, ≥99%), Poly (D,L-lactide-co-glycolide) (PLGA, lactide:glycolide=75:25, MW 66,000-107,000), Poly(vinyl alcohol) (PVA, MW 13,000-23,000, 87-89% hydrolyzed), sodium alendronate ($NaC_4H_{12}NO_7P_2 \cdot 3H_2O$), iron (III) chloride ($FeCl_3$, 97%), iron (II) chlride ($FeCl_2$ ≥98%), calcium chloride dihydrate ($CaCl_2 \cdot 2H_2O$ ≥99%), sodium oxalate (NaC_2O_4, ≥99%), sodium chloride (NaCl, ≥99%), sodium sulfate (Na_2SO_4, ≥99%), potassium phosphate monobasic (KH_2PO_4, ≥99%), gelatin from bovine skin (Type B, powder, bioreagent, suitable for cell culture), ammonium chloride (NH_4Cl, ≥99%), potassium chloride (KCl, ≥99%), sulforhodamine B ($CH_{29}N_2NaO_7S_2$, dye content 75%), fluorescein-5-isothiocyanate (FITC, $C_{21}H_{11}NO_5S$), and sucrose ($C_{12}H_{22}O_{11}$, ≥99.5%) were purchased from Sigma-Aldrich. Human embryonic kidney 293 (HEK-293, fibroblast cell) and human kidney-2 (HK-2) cell were purchased from the Korean Cell Line Bank. Polytetrafluoroethylene (PTFE, I.D.: 500 μm, O.D.: 1800 μm) tubing was purchased from Rebodix Co.. Glass capillary tubing (I.D.: 1250 μm, O.D.: 1650 μm, length: 10 cm) was purchased from Upchurch Scientific Co.. UV-curable acrylate 3D printing resin (Plas. CLEAR ver. 2.0) was purchased from ASIGA

Co.. Ethanol (C_2H_5OH, 94.5%) and deionized water (D.I. water, conductivity 18.2 mS) were purchased from Samchun Pure Chemical Co. Ltd.

Characterization

Field-emission scanning electron microscopy (FE-SEM) was performed using JSM 7401F. High-resolution transmission electron microscopy (HR-TEM) and electron energy loss spectroscopy (EELS) were performed using JEOL JEM-2100F. Optical microscopic fluorescence images were taken using Nikon Ti-DH microscope. Fourier transform infrared (FTIR) spectra were recorded using the JASCO 4600 in the range 400-4000 cm^{-1}. Uv-vis adsorption spectra were recorded on a UV-vis spectrometer (Thermo Scientific, NanoDrop 2000) in quartz cuvettes.

Preliminary calcium oxalate removal test of three chelating compounds in the flask.

The preparation of calcium oxalate (CaOx) in the flask

Before the preliminary calcium oxalate removal test, we followed the reported method to prepare calcium oxalate (CaOx), which is the main component of kidney stones[1]. For the preparation of artificial calcium oxalate as a urolithiasis simulant, 5 mL calcium chloride dihydrate (5 mM) was added to 5 mL sodium oxalate (5 mM). And then, the precipitated calcium oxalate was separated and washed several times with D.I. water using the centrifuge (4500 rpm, 10 min) and finally dried in a vacuum oven at 80 ^oC for 24 hrs [2].

Calcium oxalate (CaOx) removal efficiency test by chelating solutions

For a selection of a chelating solution to be encapsulated into the microcapsules, the calcium oxalate removal test of each chelating solution (ethylenediaminetetraacetic acid (EDTA), sodium hexametaphosphate (HMP), and citrate) was performed using the calcium oxalate powder (20-30 mg) in the Eppendorf tube (E.P. tube). The chelating solutions

(concentration: 10 mM) of EDTA, HMP, and sodium citrate were dissolved in 1000 μL PBS (pH 5.8). And then, calcium oxalate powders were added to each chelating solution (HMP, EDTA, and citrate) under the same condition (chelator concentration: 10 mM, exposure time: 30 min, chelator volume 1000 μL) in the E.P. tube. For the detailed removal test of the selected HMP solution, calcium oxalate removal tests were performed under broader conditions: concentration (1-100 mM), exposure time (1-1440 min), and volume of HMP solution (10-1000 μL).

$$Removal\ efficiency(\%) = \left(\frac{Weight\ of\ dissolved\ stone}{Initial\ stone\ weight}\right) \times 100$$

Cytotoxicity assay

The cell viability of each solution under different conditions was analyzed with HEK-293 (Human embryonic kidney 293) cell[3–6] . First, different concentrations (1, 5, 10, 50, and 100 mM) and volume (10-1000 μL) of chelating solutions (EDTA, HMP, and citrate) were prepared in DMEM (Dulbecco`s Modified Eagle Medium) supplemented with 10 % fetal bovine serum (FBS). Then the solution was separately added to a 96-well plate containing HEK-293 cell at a concentration of $2x10^4$ cells per well. After different times (1, 30, 60, and 1440 min) of incubation in a CO_2 incubator at 37 ^oC, an MTS assay was performed. Note that, all the experiments were performed in triplicate. Futhermore, human kidney-2 (HK-2) cells were also used to verify the cytotoxicity under the same concentations (1, 5, 10, 50 and 100 mM) of chelating solutions (EDTA and HMP) in RPMI (Roswell Park Memorial Institute) 1640 medium. Then the solution was separately added to a 96-well plate containing HK-2 cells at a concentration of 1×10^5 cells per well. MTT assays were performed after incubation in a CO_2 incubator at 37°C for 60 min. Note that, all the experiments were performed in triplicate [7,8].

Table S1. CaOx removal efficiency and HEK-293 cell viability of three chelating candidates (citrate, EDTA, and HMP) under the same condition (chelator concentration: 10 mM, exposure time: 60 min, chelator volume: 1000 μL) in the E.P. tube.

Types	Removal efficiency (%)	Cell viability (%)
Control (PBS 7.4)	0	100
Citrate	13	99
EDTA	25	82
HMP	**23**	**94**

Table S2. CaOx removal efficiency and HEK-293 cell viability of selected HMP solution at broader conditions (HMP concentration: 1-100 mM, exposure time: 1-1440 min, and HMP volume: 10-1000 μL) in the EP tube. When the concentration effect was studied, the conditions of exposure time 30 min and HMP volume 300 μL were fixed. For studying the effect of exposure time, the conditions (HMP concentration: 10 mM and HMP volume: 300 μL) were fixed. For the experiment on the effect of HMP volume, the conditions (HMP concentration: 10 mM and exposure time: 30 min) were fixed.

Conc.	Removal efficiency (%)	Cell viability (%)	**Exposure time**	Removal efficiency (%)	Cell viability (%)	**HMP volume**	Removal efficiency (%)	Cell viability (%)
100 mM	28	62	1440 min	34	59	1000 μL	24	-
50 mM	25	71						
10 mM	22	94	60 min	24	94	300 μL	23	94
5 mM	17	96	30 min	22	97	100 μL	19	-
1 mM	15	100	1 min	15	99	10 μL	20	-

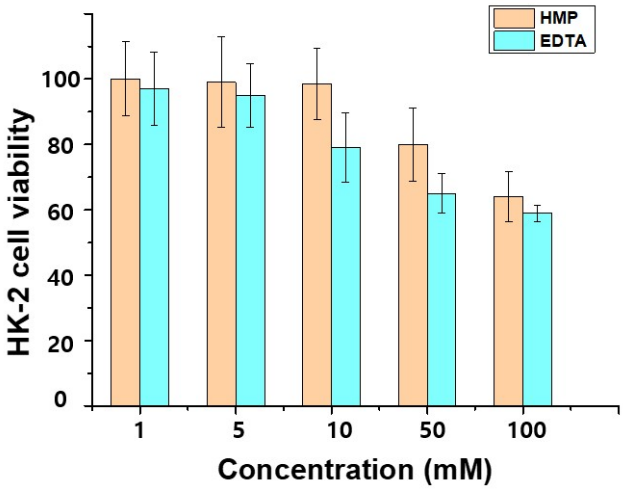

Fig. S1. Cytotoxicity test of HMP and EDTA on HK-2 cells under different concentrations (1, 5, 10, 50, and 100 mM) for 60 min of exposing time.

Fabrication of a double droplet microfluidic generator

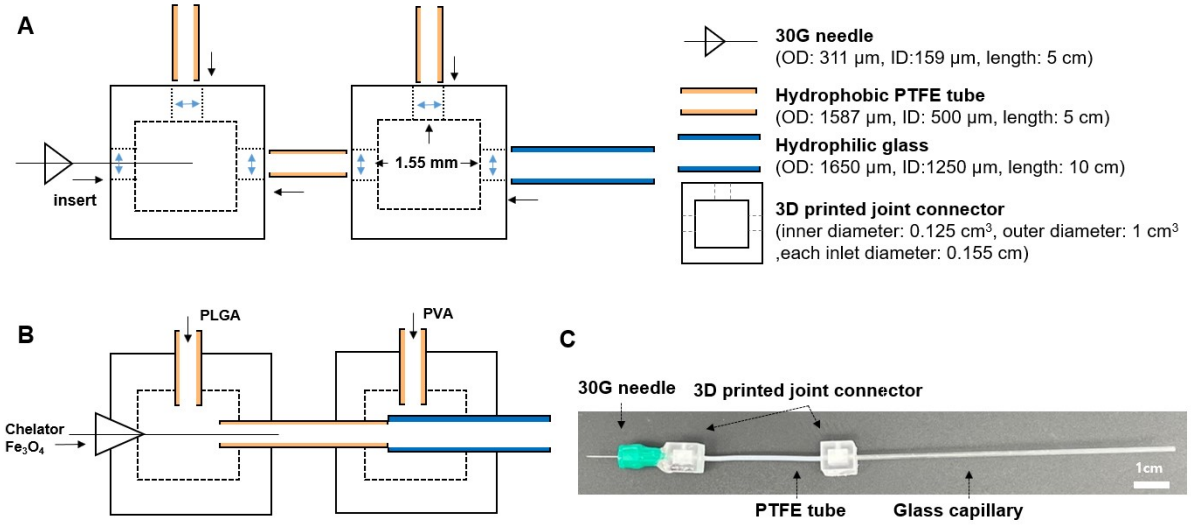

Fig. S2. (A, B) Schematic illustration of double droplet microfluidic generator, which is composed of 30G needle (OD: 311 μm, ID:159 μm, and length: 5 cm), hydrophobic PFPE tube (OD: 1587 μm, ID: 500 μm, and length: 5 cm), hydrophilic glass capillary (OD: 1650 μm, ID:1250 μm, and length: 10 cm), and hollow 2 cubics pieces of 3D printed joint connectors (inner 0.5 x 0.5 cm, outer 1 x 1 cm, wall thickness: 0.5 cm, and inlet diameter: 0.155 cm). The

30G needle was 5 cm long in total by inserting up to 3 cm in an inlet of the 3D printed joint connector. The PFPE tube was 5 cm long in total by inserting up to 4 mm in both inlet and outlet of two 3D printed joint connectors, and the glass capillary was 10 cm long in total by inserting up to 5 mm in the outlet of second part of 3D printed joint connector. (C) The actual image of a double droplet microfluidic generator (total length: 16.7 cm) to produce microcapsules.

The double droplet microfluidic generator was fabricated by modifying the reported process[2]. The double droplet generator to fabricate microcapsules is shown in Fig. S2. The droplet generator, which is composed 3D printed joint connector, 30G needle, PTFE tube, and glass capillary, was made very easily and reproducibly. 3D printed joint connectors of cubic shape were used to connect the PTFE tube and glass capilary to inject each solutions. The 30G needle was connected from the first part of 3D printed joint connector to the inside of the PTFE tube for fabricating the W/O emulsion with the middle phase (PLGA solution) and the hydrophilic glass capillary connected with the second part of 3D printed joint connector allows the formation of a highly reproducible W/O/W emulsion.

The 3D printed joint connectors were designed with auto-CAD software to create a virtual object (Autodesk inventor 2022). Then, connectors were printed with Digital Light Processing (DLP) desktop printer (Asiga Pico 2, Australia) with a UV-curable acrylate resin (Plas. CLEAR, ASIGA). Multiple digital masks were irradiated with UV (wavelengths: 385 nm and intensity: 2 mW cm^{-2}) during an exposure time of 5 sec with a set of layers 40 μm thick. Then they were washed repeatedly with isopropanol and ethanol to remove the uncured 3D printed resin. The fabricated connectors were post-treated with a UV radiation lamp with 2 mW cm^{-2} intensity for 30 min to stabilize with robust structure. The 3D printed joint connectors

have the same inner diameter (0.5 cm), outer diameter (1 cm), wall thickness (0.5 cm) and each inlet diameter (0.155 cm).

Preparation of vaarious microcapsules in flask and microfluidics

Synthesis of Fe_3O_4-citrate nanoparticle in the flask

First, we prepared Fe_3O_4-citrate nanoparticles (NPs) by slightly modifying the method of the reported process[9]. In detail, Fe_3O_4 NPs were synthesized through the co-precipitation method. $FeCl_3$ (4.44 g) and $FeCl_2$ (1.732 g) were dissolved in D.I water (80 mL) under a nitrogen atmosphere with refluxing. And then, the mixture was mechanically stirred at 1000 rpm for 30 min at 65 ^oC. In addition, the ammonia solution (20 mL) was added to the mixture. For the prevention of Fe_3O_4 NPs aggregation, sodium citrate (4 mL, 0.5 g mL^{-1}) was added to the mixture, which was stirred for 60 min at 90 ^oC. And then, the obtained Fe_3O_4-citrate nanoparticles were collected with magnet (400 mT) and washed several times with D.I. water and finally dried in a vacuum oven at 80 ^oC for 24 hrs[10–14].

Synthesis of fluorescein-5-isothiocyanate-alendronate (FITC-ALS) dye in the flask

The FITC-ALS was synthesized by slightly modifying the reported method[15]. Fluorescein isothiocyanate isomer I (FITC, 1.13 μmol) was dissolved in DMSO and then mixed with 11.3 μmol of alendronate (ALS) dissolved in bicarbonate buffer, pH 9.0. The solution was stirred (350 rpm, 2 hrs) at room temperature in the dark condition. The result solutions were dialyzed with acetate cellulose membrane (molecular cut: 12 kDa) with D.I. water for 24 hrs and dried in a vacuum oven at 80 ^oC for 24 hrs in dark condition.

Preparation of microcapsule (HMP/Fe_3O_4/S-Rh.B@PLGA) in a flask

The double emulsion type of microcapsules ($W_1/O/W_2$) in the flask was synthsized by slightly modifying the method of the previous report [16]. The mixture (W_1 phase) of HMP (10 mM), PVA (0.5 wt%), S-Rh.B (sulforhodamine B) (0.5 mM) and Fe_3O_4 NPs (1 wt%) were

prepared in D.I. water (0.1 mL). And then, the mixture was added to 4 mL DCM (O phase) containing PLGA (10 wt%), and the mixture was homogenized at 14500 rpm min^{-1} for 1 min to obtain the W_1/O emulsions. And then, the W_1/O emulsion was injected into 10 mL of PVA (10 wt%, W_2 phase) aqueous solution and emulsified at 8500 rpm min^{-1} for 10 sec, creating the W_1/O/W_2 double emulsion. The HMP/Fe_3O_4/S-Rh.B@PLGA microcapsules were collected in a vial filled with sucrose 10 wt% to prevent microcapsules from bursting by osmotic pressure. The obtained products were dispered in the sucrose 10 wt% to evaporate DCM solvent with an orbital shaker (90 rpm) for 3 hrs at room temperature. Subsequently, the microcapsules were three times with D.I. water and stored in 10 mL sucrose (10 wt%).

Preparation of microcapsule (HMP/Fe_3O_4/S-Rh.B@PLGA, Fe_3O_4/FITC-ALS@PLGA) in a double droplet microfluidic generator

The microcapsules were prepared in the double droplet microfluidic generator. The HMP (1-100 mM), S-Rh.B (10 mM) and Fe_3O_4 (0.1-1 wt%) aqueous solutions (W_1 phase) were prepared to inject into the inner phase. Moreover, the PLGA (O phase, 10 wt%) dissolved in DCM solution was injected into the middle phase to obtain the W_1/O emulsions. Finally, aqueous PVA (W_2 phase, 10 wt%) was injected into the outer phase to obtain the W_1/O/W_2 emulsions. The obtained Rh.B/HMP/Fe_3O_4@PLGA microcapsules were collected in a vial filled with sucrose 10 wt% to prevent microcapsules from bursting by osmotic pressure. Note that, since the productivity of the double droplet microfluidics generator was 8 Hz (sec^{-1}), the number of 10, 20, 100, 500 and 1000 microcapsules were obtained by operating for 1.25, 2.5, 12.5 62.5 125 sec, respectively. The obtained microcapsules immersed in sucrose 10 wt% were evaporated with an orbital shaker (90 rpm) for 3 hrs at room temperature. Subsequently, the microcapsules were three times with D.I. water and stored in 10 mL sucrose (10 wt%) [17–19]. Note that, the microcapsules containing FITC-ALS (10 mM) were prepared by replacing HMP and S-Rh.B in the above method.

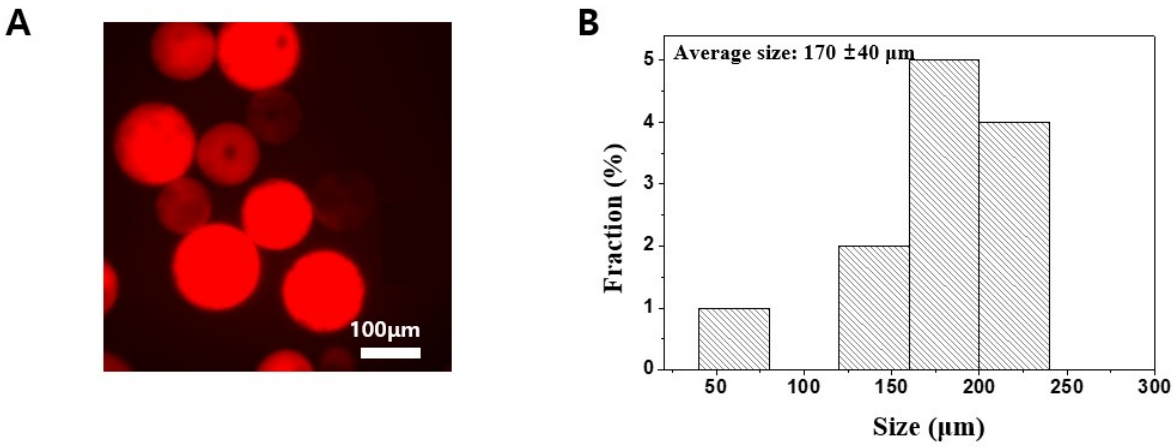

Fig. S3. (A) Optical microscope fluorescence images and (B) histography of the size distribution of microcapsules prepared by the flask.

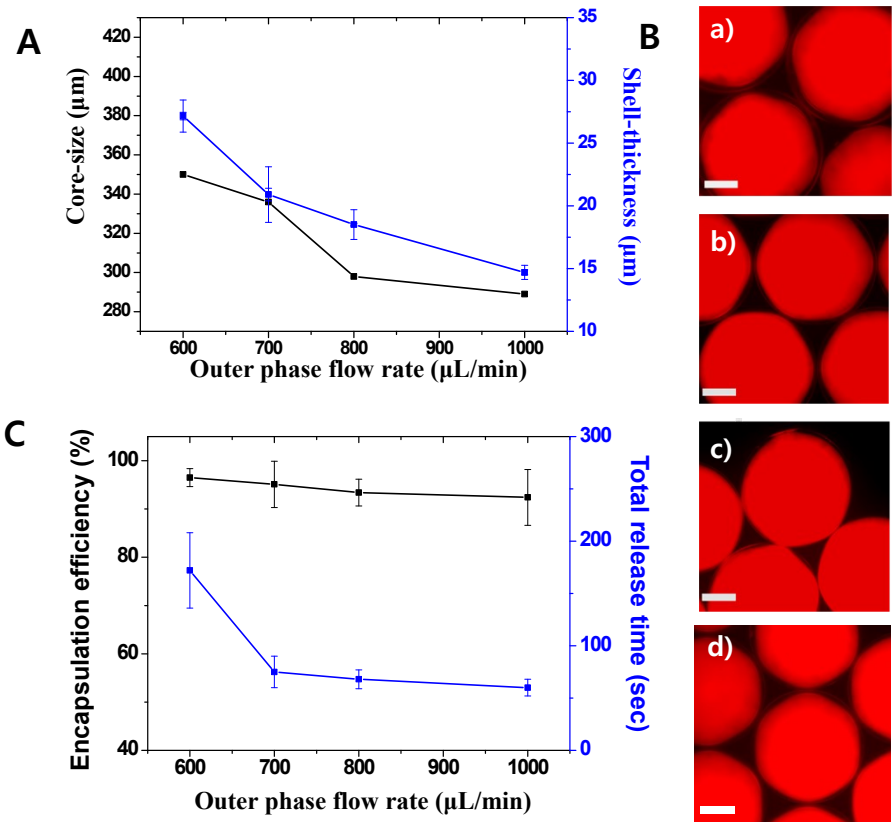

Fig. S4. Characterization of microcapsule prepared by double droplet microfluidics generator with different outer phase flow rate (600, 700, 800, 1000 μL min^{-1}). (A) A plot as well as (B) fluorescence microscopic images showing the core-shell ratio controllability of PLGA based

microcapsules by inner phase flow rate (outer phase flow rate: a) 600 μL min^{-1}, b) 700 μL min^{-1}, c) 800 μL min^{-1}, and 1000 μL min^{-1}) (scale bar: 100 μm). (C) The encapsulation efficiency of inner phase and US-responsive total release time of microcapsules at various outer phase flow rates. Note that, the outer phase flow rate was controlled with the fixed total flow rate of the inner (15 μL min^{-1}) and the middle phase (100 μL min^{-1}).

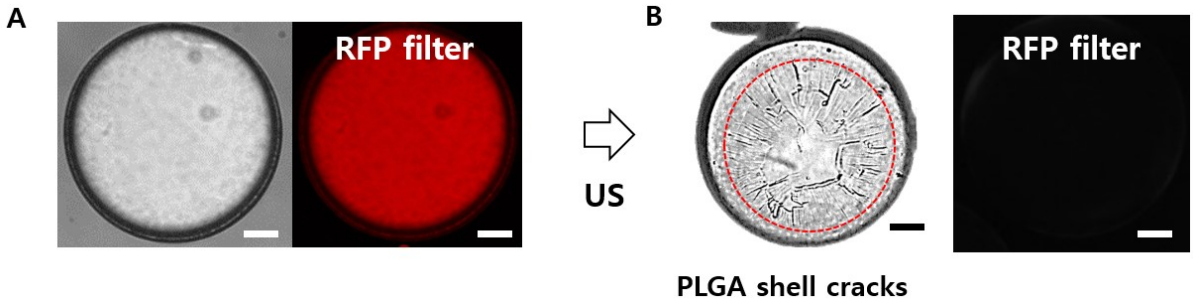

Fig. S5. Optical microscope images of microcapsules (HMP/Fe_3O_4/SRh.B@PLGA) (A) before and (B) after ultrasound exposure (US power: 50 kHz) to confirm the ultrasound responsive release of PLGA based microcapsule. Scale bar: 50 μm

The mechanism of US responsive release in some reported papers was speculated to be thermal and cavitation effects[7]. To elucidate the mechanism of our microcapsule, we confirmed the microscopic images of microcapsules before and after the US stimulation. At the microcapsules shell, the broken cavity was confirmed after US treatment for 20 sec. As a result, we expect that the thin shell of microcapsules was broken by cavitation effect.

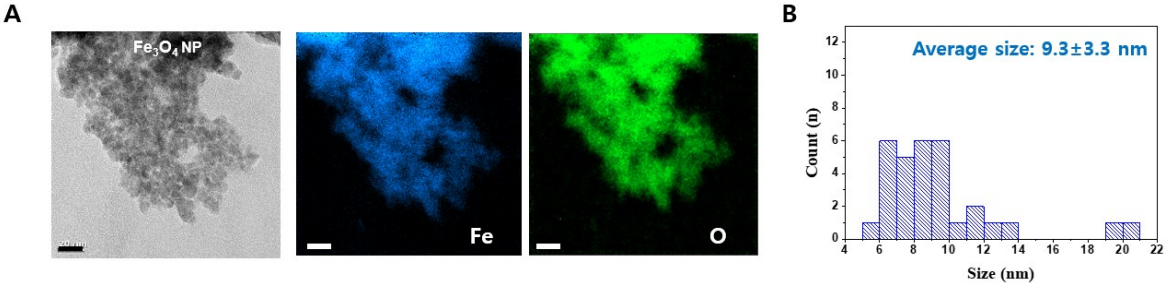

Fig. S6. (A) TEM-EELS images and (B) histogram of the size distribution of Fe_3O_4 (Scale bar: 20 nm).

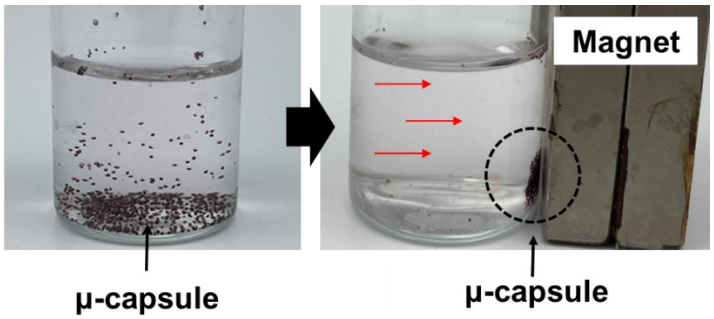

Fig. S7. left) Photographs of the dispersed microcapsule in D.I. water, and right) collected with an external magnet.

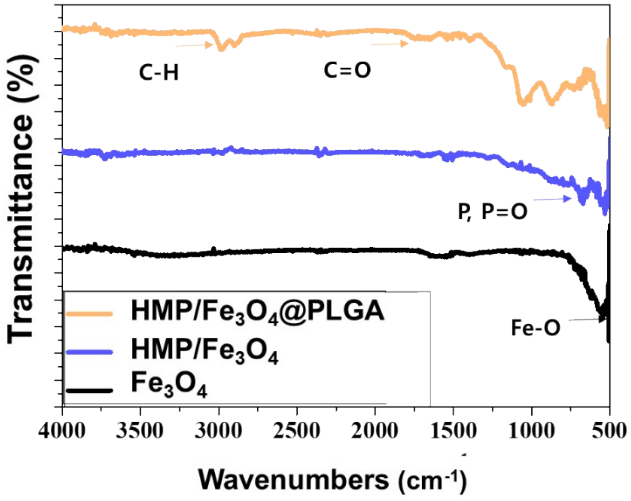

Fig. S8. FTIR spectra of Fe_3O_4 NPs (black line), HMP/Fe_3O_4 (blue line), and HMP/Fe_3O_4@PLGA (light orange line).

Measurement of encapsulation efficiency of inner phase in microcapsules

The fluorescence dye, which is S-Rh.B (λ_{ab}: 565 nm), with UV-vis absorbance was used instead of HMP to measure the encapsulation efficiency of chelating solution because

HMP solution does not have a specific UV-vis spectrum[20]. The encapsulated fluorescence S-Rh.B dye in the microcapsules was totally released by completely popping up the capsule under ultrasound irradiation for 5 min. The supernatant was collected after centrifugation at 13500 rpm for 1 min, and the amount of S-Rh.B in the supernatant was quantitatively measured using a UV-vis with an absorption wavelength 595 nm. The encapsulation efficiency was calculated by the following formula:

$$Encapsulation\ efficiency\ (\%) = \frac{Encapsulated\ concentration\ of\ aqueous\ fluorescence\ dye\ (}{Total\ injected\ the\ concentration\ of\ aqueous\ fluorescence\ dy}$$

Measurement of Encapsulation efficiency of Fe_3O_4 nanoparticles in microcapsules

The encapsulated Fe_3O_4 nanoparticles in the microcapsules were totally released by completely popping up the capsule under ultrasound irradiation for 5 min. The Fe_3O_4 was collected by magnet, removed supernatant with PLGA shell, and dried in 80 °C 24 hrs. The weight of the dried Fe_3O_4 was quantitatively measured using a high precision balance (METTLER TOLEDO ME204). The encapsulation efficiency of $Fe_3O_4$was calculated by the following formula:

$$Encapsulation\ efficiency\ (\%) = \frac{Weight\ of\ encapsulated\ Fe_3O_4}{Weight\ of\ total\ injected\ the\ Fe_3O_4}$$

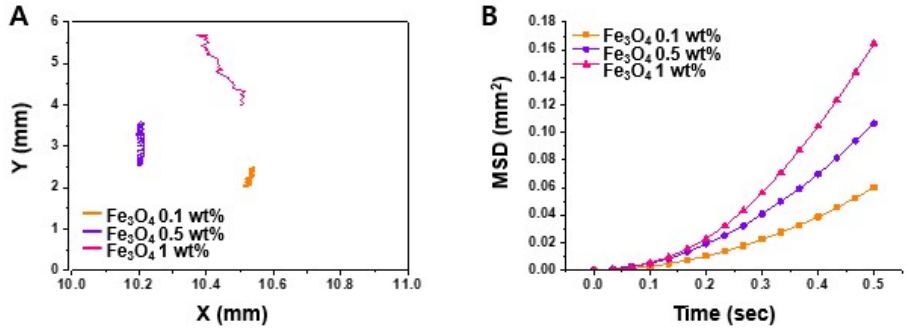

Fig. S9. Magnetic-driven motion test of the microcapsule as a micro-motor under different Fe_3O_4 concentrations (0.1, 0.5, and 1 wt%). (A) swimming trajectories and (B) mean square displacement (MSD).

Motion test of microcapsule containing different concentrations of Fe_3O_4 NPs

2D motion tracking of microcapsules (10 particles) was recorded using smartphone video (Apple iPhone 12, 1080p at 30 fps, HDP video recording with Dolby Vision) at room temperature for 20 sec. Video analysis and modeling tool Tracker 5.1.3 software was used to analyze the trajectories, calculated the mean squared displacement (MSD) and average velocity by using the aqueous dispersed microcapsules (flow rate ratio; inner:middle:outer phase =15:100:1000 μL min^{-1}) and magnetic power was 400 mT. MSD was calculated by the following formula. $$MSD(\Delta t) = \ < r2(\Delta t) >= \left\langle \frac{1}{N}\sum_{i=0}^{N}\left[r_i(t) - r_i(t+\Delta t)\right]^2 \right\rangle$$ N: number of particles, $r_i(t) - r_i(t+\Delta t)$ vector distance traveled by a particle over the time (Δt) interval.

Magnetic collection efficiency of the microcapsules prepared by microfluidics and flask

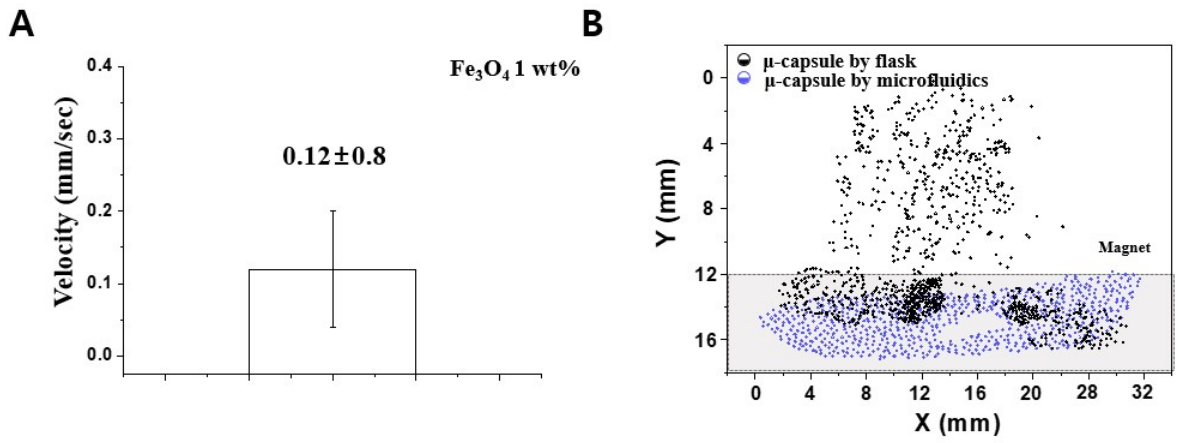

Fig. S10. Comparative magnetic collection efficiency of two types of microcapsule prepared by flask and droplet microfluidic generator. Note that, the initial microcapsules were placed

within 0-4 mm of Y-axis and the magnet was placed on the 12-16 mm of Y-axis. (Y-axis 1=1 mm). (A) The velocity of microcapsules prepared in a flask and (B) trajectories of two types of microcapsules made by flask and microfluidics droplet generator to determine the distribution when magnetic field (400 mT) was applied for 2 min.

For magnetic collection efficiency, microcapsules (>500 capsules) prepared by the flask and microfluidics were located within the Y-axis (0-4) of the microscope coordinates. After that, a magnet (400 mT) was placed on the Y-axis (12-18), and the collection of microcapsules was taken with a coordinate of the Y-axis (12-18) for 2 min. The number of microcapsules moved more than 8 mm from the initial position to the magnet position was compared. Video analysis of the microcapsules Image J software was used. The magnetic collection efficiency was calculated by the following formula:

$$Magnetic\ collection\ efficiency\ (\%) = \left(\frac{Magnetic\ attrected\ the\ number\ of\ \mu\_capsule\ of\ above\ Y\ axis\ (0-4)}{Total\ the\ number\ of\ \mu\_capsule}\right) \times 100$$

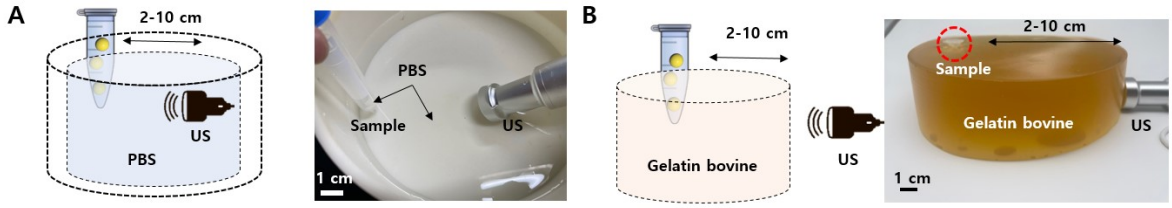

Fig. S11. Schematic illustration and actual images of experimental set-up for investigating the dependence of ultrasound responsive release behavior on (A) low dense PBS (pH 5.8) and (B) high dense gelatin as human body mimics.

The body tissue mimics gelatin for testing the ultrasound responsive solution release time was prepared by reported method[21]. First, the aqueous dispersed gelatin (20 wt%) was

added to round shape container and irradiated for 20 min in the microwave (KR-B202WL, 700W, 2450 MHz) and transferred to a refrigerator for 24 hrs at 4°C.

Removal test of artificial CaO_X stone in a Ψ-shaped flow chip

Fabrication of Ψ-shaped flow chip by imprinting method.

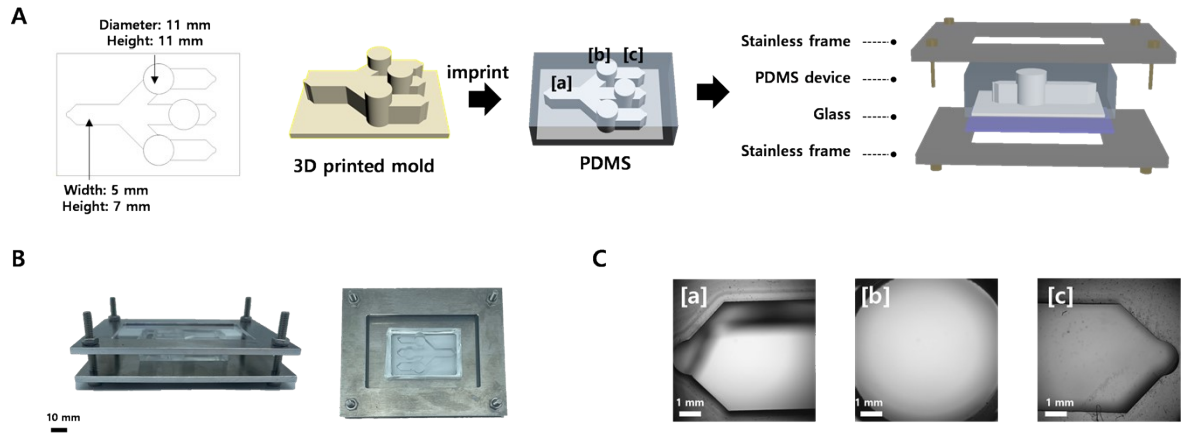

Fig. S12. (A) Schematic images of fabricating the flow chip designing the Ψ-shaped flow chip by AutoCAD, fabrication of polymer mold by 3D printing, c) PDMS imprinting of the Ψ-shaped flow chip, and clamping of flow chip and stainless frame, (B) actual images, and (C) microscope images of [a-c] region of flow chip to test the stone removal.

The Ψ-shaped flow chip was prepared by PDMS imprinting method. The Ψ-shaped PMMA mold (45x30 mm) and stainless frames (100x80 mm) were designed using 3D-CAD software and the designed Ψ-shaped PMMA mold was printed by 3D printer. And then, we prepared the Ψ-shaped flow chip by pouring the PDMS solution (PDMS: curing agent =10:1) into a Ψ-shaped PMMA mold in the petri dish (150x25 mm) and curing the PDMS in an oven at 80 °C for 3 hrs. The upper and lower parts of the frames were manufactured separately by CNC processing using a CTX Beta 1250 TC (DMG MORI). Finally, the PDMS-based flow chip was tightened by upper and lower parts with hexagonal screws to conduct the stone removal experiments.

Preparation of artificial urine.

The artificial urine was prepared using reported method[2]. The calcium chloride dihydrate (1.103 g), sodium chloride (2.925 g), sodium sulfate anhydrous (2.25 g), potassium phosphate monobasic (1.4 g), potassium chloride (1.6 g), ammonium chloride (1 g), urea (25 g), and creatinine (1.1 g) were dissolved in D.I. water (1 L). The final artificial pH was 5.8.

Table 3. The dependence of HMP retention time on counter flow rate (0.125-1 mL min^{-1}), the number of microcapsules (10-1000), and HMP concentration (10-100 mM) in a flow chip.

	Sum of flow rate (mL/min)								
	0.125			0.5			1		
Number (N) / Conc. (mM)	10	100	1000	10	100	1000	10	100	1000
10	15 min	15.5 min	16.3 min	3.4 min	3.4 min	3.8 min	1.2 min	1.5 min	2.2 min
50	16.6 min	16.8 min	17.3 min	3.8 min	3.9 min	4.3 min	2 min	2.3 min	2.8 min
100	17.3 min	17.5 min	18.5 min	4.3 min	4.5 min	**4.9 min**	2 min	2.4 min	3.1 min

Delivery efficiency of microcapsule in the flow chip

The magnetic-guided delivery efficiency of microcapsules (ALS-FITC/Fe_3O_4) was analyzed in the dynamic urine flow condition (0.5 mL min^{-1}) of the flow chip. First, we placed the CaOx stone in the flow chip ([c] region; placed magnet). And then, the prepared microcapsules (number of microcapsules>20) were supplied into flow chips. Finally, we calculated the delivery efficiency by the following formula:

$$\left(\frac{The\ number\ of\ magnetic\ delivered\ microcapsules}{Total\ the\ number\ of\ supplied\ microcapsules}\right) \times 100$$

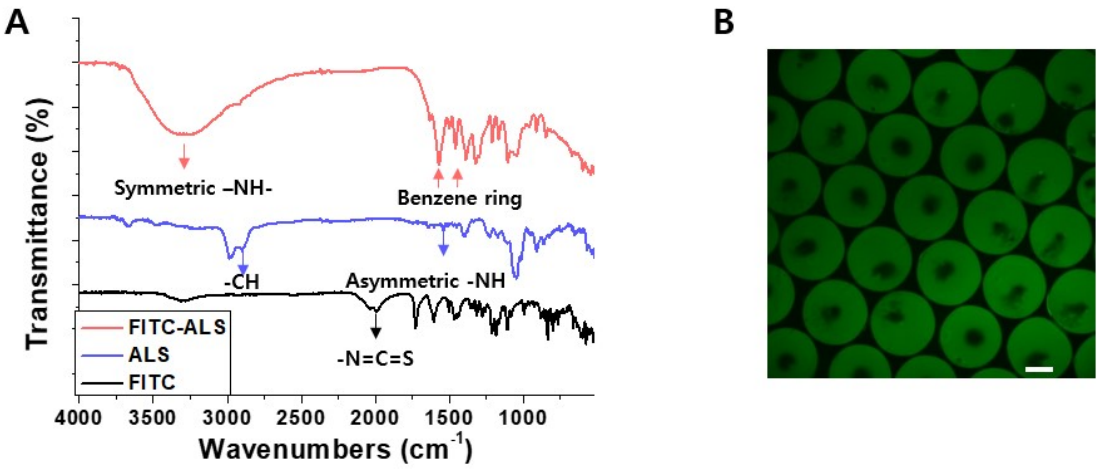

Fig. S13. Potential visualization of urolithiasis by microcapsule contatining ALS-FITC. (A) FTIR of FITC, ALS, and FITC-ALS. (B) Microscopic image of microcapsules contaning ALS-FITC and Fe_3O_4.

The FTIR spectroscopy showed that the peak at 2019 cm^{-1} corresponding to –N=C=S of FITC, the absorption peak at 1641 and 2985 cm^{-1} corresponding to asymmetric –NH and –CH, and FITC conjugated with ALS was confirmed by a new peak of the broad symmetric –NH- at 3452 cm^{-1}[115].

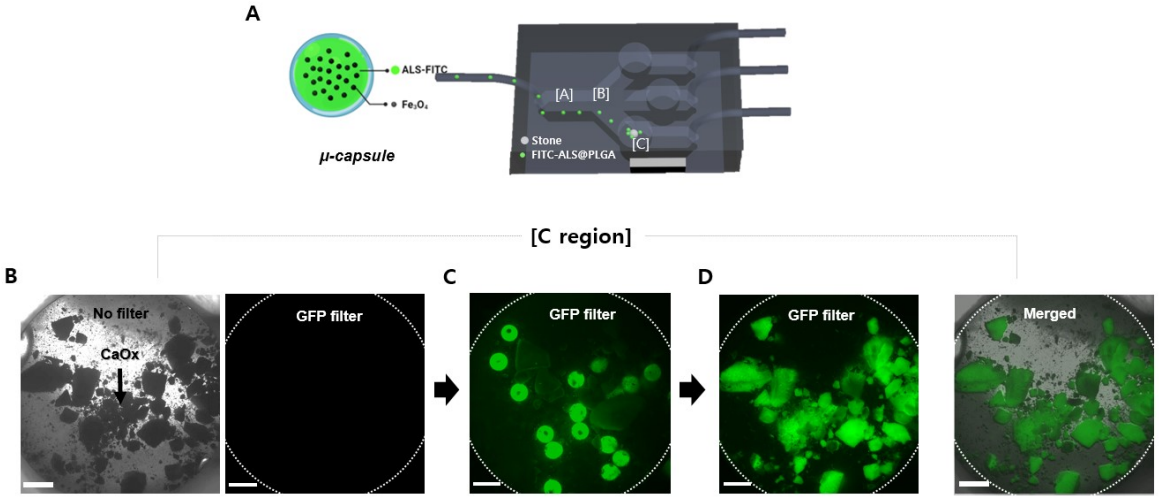

Fig. S14. (A) The scheme of staining visualization of calcium oxalate by microcapsule containing ALS-FITC/Fe_3O_4. Microscopic fluorescence image of (B) calcium oxalate stone, (C) mixed phase of microcapsules containing ALS-FITC with stone, and (D) stained calcium oxalate stone by ALS-FITC of microcapsules with US. Green colors represent the ALS-FITC, and the scale bar is 500 μm.

Experimental set-up for removing the human kidney stone in a kidney urinary flow-imitated chip.

Fabrication of PDMS based kidney urinary flow-imitated chip

We designed the PDMS-based kidney urinary flow-imitated chip using 3D CAD software by following the reference of actual human urinary tract shape and length[22]. The detailed specifications are ureter (length: 85 mm and width: 4.7 mm), renal pelvis (length: 27 mm and width: 5.3-20.2 mm), major calyx (length: 11.2-16.5 mm and width:114-16.3 mm), minor calyx (length: 10.3-15mm, width: 7.7-9.9 mm), and total kidney size (length: 66 mm, width: 135 mm. and height: 40 mm). And then, designed kidney urinary flow-imitated chip mold was printed using polymer resin (Accura 25 of Korea technology) by the SLA proX 800 printer. And then, the PDMS solution (PDMS: curing agent =10:1) was poured into 3D printed mold in the round pot (radius 90 mm, height: 100 mm) and curing the PDMS in an oven at 80 ^{o}C for 3 hrs. Finally, the kidney urinary flow-imitated chip with open space was used for human kidney stone removal test.

Preparation of artificial calcium oxalate (CaOx) stone spheres as a urolithiasis simulant

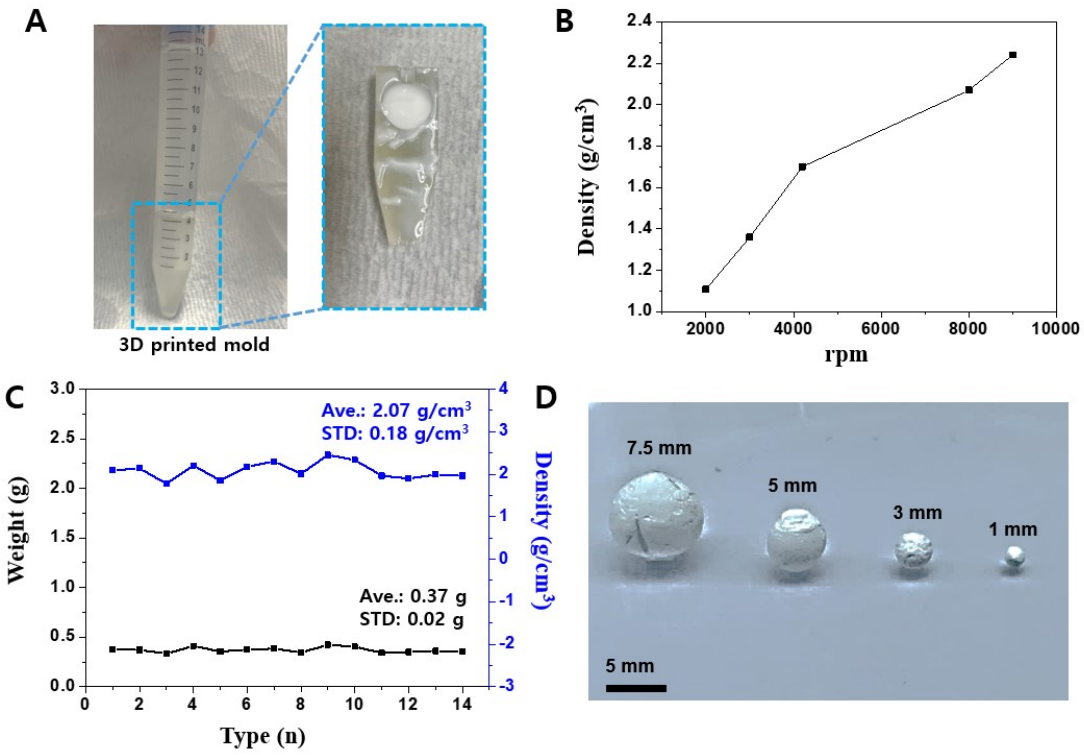

Fig. S15. The fabrication of spherical calcium oxalate stone by 3D printed mold and centrifugation. (A) Actual images of conical tubes where 3D printed mold with spherical cavities was placed. (B) The density control of calcium oxalate stone by centrifugate speed. (C) Reproducibility of optimized stone density (2.07 g/cm^3). (D) Actual image of optimized stone ㅜwith different sphere CaOx stone sizes (1, 3, 5, and 7.5 mm).

For the preparation of spherical calcium oxalate stone, the 3D printed mold with each sphere cavity (size: 1.36 mm for 1 mm stone, 4.08 mm for 3 mm stone, 6.8 mm for 5 mm stone, and 10.2 mm for 7.5 mm stone) was designed using 3D-CAD software. Note that, the stone size was controlled by sphere cavity of 3D printed mold. And then, the 3d printed PMMA mold was placed in a conical tube (15 mL for 1-5 mm size of stone or 50 mL for 7.5 mm size of stone). Next, the aqueous dispersed calcium oxalate solution (20 wt%) was poured into a 3D printed mold-equipped conical tube and centrifuged at a different speed (2000-9000 rpm) to control the calcium oxalate density[23].

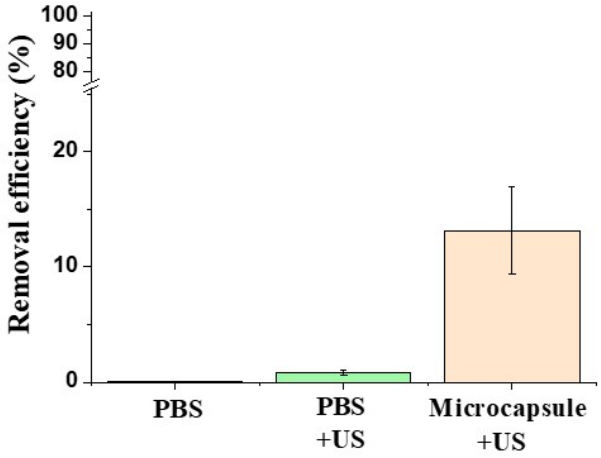

Fig. S16. Control experiment for artificial stone (5 mm) removal in the only PBS, PBS with US, and microcapsules with US in a flow chip.

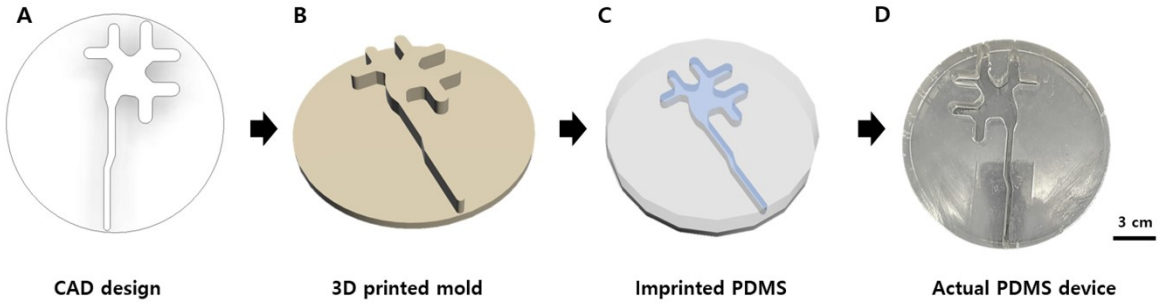

Fig. S17. Schematic images of fabricating the PDMS based kidney urinary flow-imitated chip. (A) Designing the kidney urinary flow-imitated chip by AutoCAD, (B) fabrication of 3D printed polymer mold, (C) PDMS imprinting of kidney urinary flow-imitated chip. (D) Actual image of fabricated PDMS based kidney urinary flow-imitated chip.

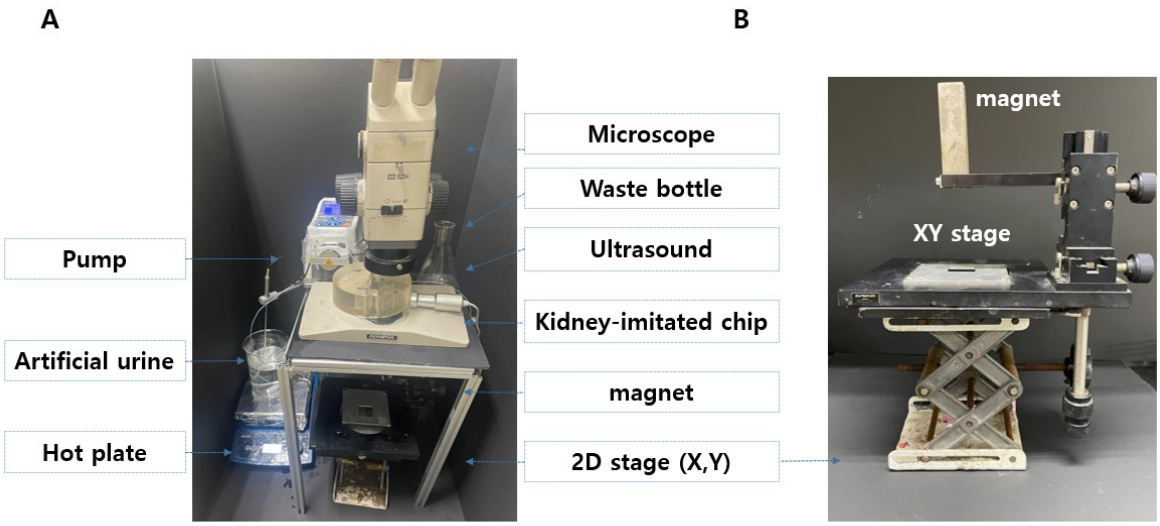

Fig. S18. Actual images of (A) experimental set-up for sequential magnetic guidance movement, US-responsive release, and removal test of microcapsules using the human kidney stone. (B) XY stage with equipped magnet for magnetic guidance movement.

For magnetic guidance movement, US-responsive release, and removal test of human kidney stone by the microcapsules, the experimental set-up was prepared. Actual human kidney stone was intentionally placed in the minor calyx of PDMS-based kidney urinary flow-imitated chip. Thereafter, the prepared artificial urine fluid (36.5 ^{o}C) was flowed in outward direction at above the human kidney stone and continuously flowed at a flow rate of 0.5 mL min^{-1} by a pump (Reglo digital gear pump of Revodix). In addition, to make a magnetic guidance mobility of the microcapsule, the magnet was equipped to the XY stage. Finally, we placed a kidney urinary flow-imitated chip on the microscope to observe the magnetic guidance movement of the microcapsule, US-responsive releasing the solution from microcapsules, and the removal of urolithiasis experiment. Note that, Considering the distance between the human abdomen and the kidney stone, the distance of stone from external stimuli (US and magnet) was set at 8 cm.

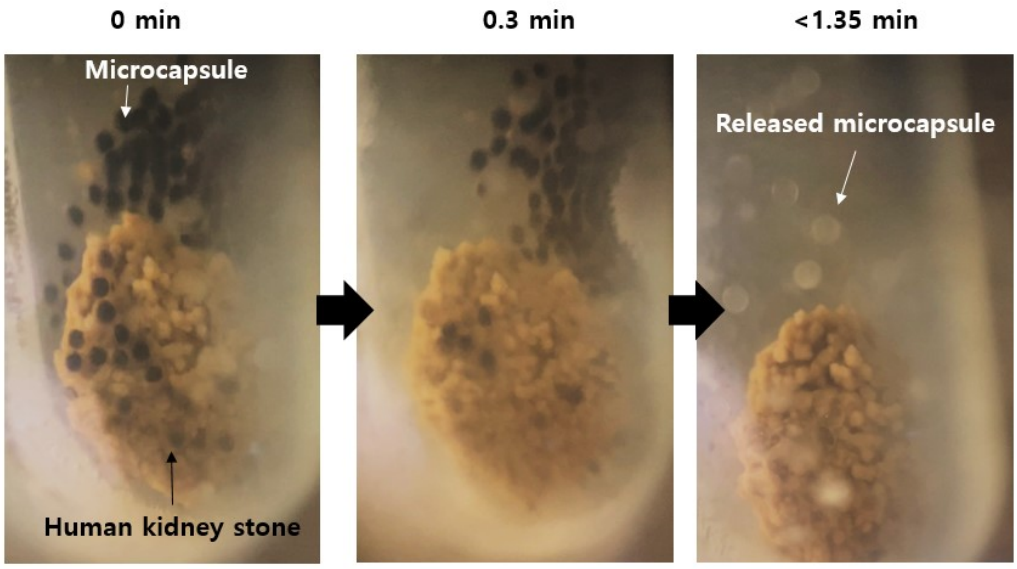

Fig. S19. Microscopic images for confirming the US-responsive releasing behavior of microcapsules. The microcapsules were released completely within 1.35 min by US (50 kHz)

Statistical analysis

All experiments were obtained from the independent experiment, at least in triplicate. All data were expressed as mean ± standard deviation.

References

1 S. Vijayan and M. Hashimoto, *RSC Adv.*, 2019, **9**, 2822–2828.

2 T. E. Robinson, T. E. Robinson, E. A. B. Hughes, O. J. Wiseman, S. A. Stapley, S. C. Cox and L. M. Grover, *J. Mater. Chem. B*, 2020, **8**, 5215–5224.

3 M. Inada, G. Izawa, W. Kobayashi and M. Ozawa, *Int. J. Mol. Med.*, 2016, **37**, 1521–1527.

4 A. A. Stepanenko and V. V. Dmitrenko, *Gene*, 2015, **569**, 182–190.

5 J. C. Liu, P. H. Lerou and G. Lahav, *Trends Cell Biol.*, 2014, **24**, 268–274.

6 A. Albert, V. Tiwari, E. Paul, D. Ganesan, M. Ayyavu, R. Kujur, S. Ponnusamy, K. Shanmugam, L. Saso and S. Govindan Sadasivam, *J. Enzyme Inhib. Med. Chem.*, 2017, **32**, 426–433.

7 W. Zhipeng, L. Li, M. Qibing, L. Linna, R. Yuhua and Z. Rong, *J. Toxicol. Sci.*, 2006, **31**, 61–70.

8 M. J. Ryan, G. Johnson, J. Kirk, S. M. Fuerstenberg, R. A. Zager and B. Torok-Storb, *Kidney Int.*, 1994, **45**, 48–57.

9 M. A. Dheyab, A. A. Aziz, M. S. Jameel, O. A. Noqta, P. M. Khaniabadi and B. Mehrdel, *Sci. Rep.*, 2020, **10**, 10793.

10 N. Tran and T. J. Webster, *J. Mater. Chem.*, 2010, **20**, 8760–8767.

11 N. Malhotra, J. S. Lee, R. A. D. Liman, J. M. S. Ruallo, O. B. Villaflore, T. R. Ger and C. Der Hsiao, *Molecules*, 2020, **25**, 1–26.

12 S. Correia Carreira, L. Walker, K. Paul and M. Saunders, *Nanotoxicology*, 2015, **9**, 66–78.

13 G. Zhou, J. Zhang, C. Pan, N. Liu, Z. Wang and J. Zhang, *Molecules*, 2017, **22**, 1–13.

14 M. S. Birajdar, H. Joo, W. G. Koh and H. Park, *Biomater. Res.*, 2021, **25**, 1–14.

15 Y. Li, Y. Li, Y. Li, Y. Fu, Y. Fu, Y. Fu, H. Zhang, H. Zhang, H. Zhang, J. Song, J. Song, J. Song, S. Yang, S. Yang and S. Yang, *Biomed Res. Int.*, 2020, **2020**, 4012194.

16 S. bin Feng, D. hao Fu, L. Nie, P. Zou and J. ping Suo, *Chinese J. Polym. Sci. (English Ed.*, 2015, **33**, 955–963.

17 J. L. Chen, M. K. Yeh and C. H. Chiang, *J. Food Drug Anal.*, 2004, **12**, 291–298.

18 R. Liu, G. Ma, F. T. Meng and Z. G. Su, *J. Control. Release*, 2005, **103**, 31–43.

19 W. Si, Q. Yang, Y. Zong, G. Ren, L. Zhao, M. Hong and Z. Xin, *Ind. Eng. Chem. Res.*, 2021, **60**, 9196–9205.

20 B. Balcomb, M. Singh and S. Singh, *ChemistryOpen*, 2015, **4**, 137–145.

21 B. G. Rock, A. P. Leonard and S. J. Freeman, *Br. J. Radiol.*, 2010, **83**, 612–614.

22 P. Wadekar and S. Gangane, *J. Coll. Med. Sci.*, 2013, **8**, 17–21.

23 O. Y. Perk, M. Şeşen, D. Gozuacik and A. Koşar, *Ann. Biomed. Eng.*, 2012, **40**, 1895–1902.